Elementary Events Underlying Voltage-Dependent G-Protein Inhibition of N-Type Calcium Channels

Parag G. Patil,* Marita de Leon,* Randall R. Reed,# Stefan Dubel,§ Terry P. Snutch,§ and David T. Yue*
*Program in Molecular and Cellular Systems Physiology, Department of Biomedical Engineering, and #Departments of Neuroscience and Molecular Biology and Genetics, and Howard Hughes Medical Institute, Johns Hopkins University School of Medicine, Baltimore, Maryland 21205 USA, and §Biotechnology Laboratory, University of British Columbia, Vancouver, British Columbia V6T 1Z3, Canada

ABSTRACT Voltage-dependent G-protein inhibition of N-type calcium channels reduces presynaptic calcium entry, sharply attenuating neurotransmitter release. Studies in neurons demonstrate that G-proteins have multiple modulatory effects on N-type channels. The observed changes may reflect genuine complexity in G-protein action and/or the intricate interactions of multiple channels and receptors in neurons. Expression of recombinant M2-muscarinic receptors and N-type channels in HEK 293 cells allowed voltage-dependent inhibition to be studied in isolation. In this system, receptor-activated G-proteins had only one effect: a 10-fold increase in the time required for channels to first open following membrane depolarization. There were no changes in gating after the channel first opened, and unitary currents were not detectably altered by modulation. Despite its simplicity, this single change successfully accounts for the complex alterations in whole-cell current observed during G-protein inhibition in neurons.

INTRODUCTION

N-type voltage-activated Ca^{2+} channels transduce action potentials into presynaptic Ca^{2+} entry, triggering neurotransmitter release from a wide variety of nerve terminals (Dunlap et al., 1995). Because Ca^{2+} entry through even a single open channel may initiate release (Stanley, 1993), selective modulation of N-type channels constitutes a potent mechanism for spatio-temporal control of synaptic transmission. The dominant form of N-type channel modulation, and a key component of presynaptic inhibition (Miller, 1990) and opiate analgesia (Wilding et al., 1995; Bourinet et al., 1996), is voltage-dependent inhibition by receptor-coupled G-proteins. While much work argues that voltage-dependent inhibition results from direct binding of G-proteins to N-type channels (Wickman and Clapham, 1995; Hille, 1994), the functional effects of G-proteins on the operation of the channel remain unclear and are subject to debate. Studies in neurons suggest that G-proteins produce multiple changes in the pattern of opening and closing (gating) of the channel. Studies of macroscopic, whole-cell currents (Bean, 1989; Kasai and Aosaki, 1989; Elmslie et al., 1990; Pollo et al., 1992; Boland and Bean, 1993) propose that G-proteins increase the time required for a channel to first open after membrane depolarization (first latency). Surprisingly, studies of single-channel currents, which should directly resolve the effects of G-proteins on channel gating, point to a different mechanism. One single-channel study of voltage-dependent G-protein inhibition in neurons (Delcour and Tsien, 1993) suggests that G-proteins alter the prevalence of three distinct gating patterns, called "modes," which have distinct open and closed times but *similar* first latencies. By contrast, another single-channel study (Carabelli et al., 1996) suggests that G-proteins not only slow first latencies but also affect open and closed times after the channel first opens. In addition to altered gating, the suggestion that the flux of Ca^{2+} ions through open channels (unitary current) may be subject to modulation introduces further complexity into the mechanism of voltage-dependent G-protein inhibition. Fluctuation analysis of whole-cell currents in neurons (Kuo and Bean, 1993) suggests that nearly half of G-protein inhibition may be attributable to a reduction in unitary current. Such an effect has yet to be confirmed by direct measurements at the single-channel level. If proven to be correct, voltage-dependent G-protein inhibition would represent one of the rare instances of ion channel modulation by changes in permeation as well as in gating (Chen and Huang, 1992). In short, multiple functional effects of G-proteins on N-type channels have been reported, but few have been uniformly established.

The lack of consensus on the mechanism underlying voltage-dependent G-protein inhibition may derive, in part, from the heterogeneity of Ca^{2+} channel and receptor populations in neurons. In whole-cell studies, other Ca^{2+} channels could contaminate native N-type currents, potentially obscuring the effects of G-proteins on N-type channels. In single-channel studies, a particular Ca^{2+} channel type might be misidentified as another (Elmslie et al., 1994). Furthermore, in neurons, a single receptor agonist may stimulate multiple modulatory pathways that converge on N-type channels (Bernheim et al., 1991; Luebke and Dunlap, 1994). It may therefore prove to be quite challenging to differentiate observed effects from one pathway or another.

To circumvent the challenges of heterogeneity, we co-expressed a recombinant M2-muscarinic receptor and an

Received for publication 24 May 1996 and in final form 2 August 1996.

Address reprint requests to Dr. David T. Yue, Program in Molecular and Cellular Systems Physiology, Department of Biomedical Engineering, Johns Hopkins University School of Medicine, 720 Rutland Avenue, Baltimore, MD 21205. Tel.: 410-955-0079; Fax: 410-955-0549; E-mail: dyue@bme.jhu.edu.

0006-3495/96/11/2509/13 $2.00

N-type Ca^{2+} channel in HEK 293 cells, enabling single-channel study of an isolated pathway of voltage-dependent G-protein inhibition of purely N-type channels. In contrast to the multiple effects suggested by neuronal studies, our reconstituted system revealed that a single change in gating underlies voltage-dependent inhibition of N-type channels. Only delays in the time to first opening following membrane depolarization were observed with inhibition. After the first opening, there were no changes in open or closed times, as gauged by conditional open-probability analysis. Furthermore, inhibition produced no change in unitary current amplitude, as measured by bootstrap amplitude histogram analysis.

MATERIALS AND METHODS

Expression of recombinant receptors and channels

Complementary DNAs encoding an M2 receptor (Peralta et al., 1987), and channel subunits α_{1B} (rbB-II: Dubel et al., 1992), β_{1b} (Pragnell et al., 1991), and α_2 (Tomlinson et al., 1993) were subcloned into CMV-promoter expression plasmids. HEK 293 cells were transfected as described (Dhallan et al., 1990) with 0.5, 3, 1, and 12 μg of each plasmid, respectively, per 100-mm plate. Untransfected HEK 293 cells contain no detectable high voltage-activated calcium channels. In three rounds of transfections with the calcium channel β_{2a} subunit alone, we screened over 40 cells and found none with detectable high-threshold calcium current. Binding assays detect insignificant numbers of endogenous muscarinic receptors in HEK 293 cells (Peralta et al., 1988).

Electrophysiology

Whole-cell currents were recorded at room temperature by patch-clamp techniques with an Axopatch 200A (Axon Instruments, Foster City, CA). The bath solution contained 10 mM $BaCl_2$, 140 mM tetraethylammonium methanesulfonate (TEA-$MeSO_3$), and 10 mM HEPES (pH 7.4), adjusted with TEA-OH. Where noted, 50 μM carbachol (saturating dose) was included. Internal solution contained 135 mM Cs-$MeSO_3$, 5 mM CsCl, 10 mM EGTA, 1 mM $MgCl_2$, 4 mM MgATP, and 10 mM HEPES (pH 7.3), adjusted with CsOH. Where noted, 300 μM Li-GTPγS was included. Series resistance was typically <10 MΩ and was compensated by 60–80%. Leak and capacitance currents were subtracted by a P/8 protocol. Voltage pulses were delivered every 15 to 30 s; data were sampled at 10 kHz and filtered at 2 kHz (-3 dB, 4-pole Bessel), except as noted.

Single-channel currents were recorded at room temperature by on-cell patch clamp, as described (Imredy and Yue, 1994). Bath solution consisted of 132 mM K-glutamate, 5 mM KCl, 5 mM NaCl, 3 mM $MgCl_2$, 2 mM EGTA, 10 mM glucose, and 10 mM HEPES (pH 7.3), adjusted with KOH. Pipette solution consisted of 140 mM $BaCl_2$, 50 μM carbachol (where indicated) and 10 mM HEPES (pH 7.4), adjusted with TEA-OH. Voltage pulses were delivered every 5 s. The integrating headstage of Axopatch 200A was used. Data were sampled at 10 kHz and filtered at 2 kHz (-3 dB, 4-pole Bessel), except where noted.

Analysis of single-channel gating

p-Values were determined by two-sided t-test throughout, except where noted. Statistical significance was defined as $p < 0.05$. Ensemble average current and FL were calculated as described (Imredy and Yue, 1994). Average open time was determined by maximum-likelihood fits of a single exponential curve to open time distributions. The first few bins were omitted from analysis to avoid distortion by events near the dead time. Conditional open probabilities were calculated as described (Imredy and Yue, 1992), with modifications: the start of the conditioning window was set to the beginning of the test pulse, so that the first open point in the window (at time t_j) corresponded to the first opening in the trace. In multichannel patches, we exploited the expression: $E_{oo}(t, t_j) = P_{oo}(t, t_j) + (N - 1)\, P_o(t, t_j)$; where $E_{oo}(t, t_j)$ is the expected number of open channels at time t, given that the first opening in the N-channel patch occurred at time t_j. $P_{oo}(t, t_j)$ is the probability that a channel is open at time t, given that it first opened at time t_j. $P_o(t, t_j)$ is the probability that a channel is open at time t, given that it did not open up to time t_j. The main improvement in this study is use of $P_o(t, t_j)$, instead of unconditional open probability. To reduce computational requirements, $P_o(t, t_j)$ was approximated by $P_o(t, x)$, where x was the closest of 20 exponentially distributed time points in the test pulse. Simulation revealed that this approximation had no effect on the estimate of P_{oo}.

Kinetic modeling of single-channel gating events

Smooth fits in Fig. 4 were calculated through Euler integration of differential equations arising from the model in Fig. 7 *B*. Model parameters were estimated by least-squares fit of P_o, FL, and P_{oo} functions to carbachol data (Fig. 4, *B* and *D*), using the Nelder-Mead Simplex algorithm. Fits to data without carbachol (Fig. 4, *A* and *C*) resulted from visual adjustment of two parameters, the fraction of active channels and f_W (as defined, Fig. 7 *B*), while holding all other parameters constant.

For amplitude histogram sensitivity analysis (Fig. 6), a simplified version of the model in Fig. 7 *B*, lacking states C_1 and C_1', was used. Parameters were determined as above. Optimal rate constants were (in ms^{-1}): k22′ = 0; k2′2 = 0.00437; k23 = 0.161; k32 = 0.257; k34 = 0.880; k43 = 1.67; k45 = 0.041; k54 = 0.00146. The fraction of active channels starting the test pulse in state C_2 vs. C_2' was 0.28 without prepulse, and 0.89 with prepulse. The fraction of active channels was 0.75. Unitary current of channels starting in C_2' was 25% less than that of channels starting in C_2.

Analysis of single-channel permeation

Single-channel currents (Fig. 6) were recorded as described above, except that the pipettes were filled with whole-cell bath solution, containing 10 mM $BaCl_2$. Data were sampled at 10 or 25 kHz and filtered at 2 or 5 kHz (-3 dB, 4-pole Bessel), respectively. Analog filtering between 2 and 5 kHz was digitally compensated to 5 kHz (-3dB, 4-pole Bessel) using a double-precision FFT filtering algorithm (MATLAB, The Math Works, Natick, MA). Wide bandwidth and compensation largely eliminated bias introduced by incompletely resolved opening transitions (Yellen, 1984).

Amplitude histogram analysis was performed as described in the text. Estimates of unitary current amplitude derived from "active region" histograms were far more accurate than those derived from all-points histograms, because of the low open probability of N-type channels (e.g., Fig. 4). Histogram bin width was 10 fA. Confidence intervals for estimates of unitary current (i) were obtained using bootstrap methods (Efron and Tibshirani, 1993; Stricker et al., 1994). Briefly, each bootstrap estimate of i was calculated from a data set of test-pulse current records obtained by randomly sampling, with replacement, all current records (either with or without prepulse) for a patch. Repeated application of this procedure provided $n \geq 300$ bootstrap estimates of i for each patch. These estimates were normally distributed, allowing confidence intervals to be calculated from standard errors.

RESULTS

Reconstitution of an isolated pathway of voltage-dependent G-protein inhibition

Fig. 1 (*left*) shows whole-cell currents through recombinant N-type channels expressed in HEK 293 cells. When recom-

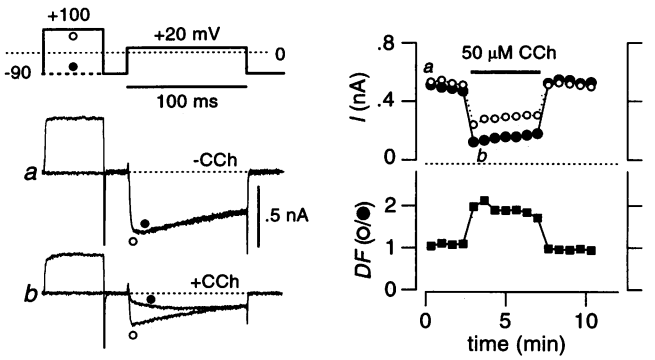

FIGURE 1 Carbachol-induced inhibition of recombinant N-type Ca^{2+} channels in HEK 293 cells. (*Left*) voltage protocol and whole-cell currents, elicited with (○) and without (●) prepulse depolarization (*Vp* = 100 mV). The prepulse and interpulse lasted 50 ms and 20 ms, respectively. Records labeled *a* and *b* were obtained without and with carbachol (CCh) in the bath, respectively. (*Top right*) diary plot of peak current during test pulses to 20 mV with (○) and without (●) a prepulse. Letters *a* and *b* in the diary plot correspond to the times at which exemplar traces *a* and *b* on the left were obtained. (*Bottom right*) diary plot of degree of facilitation (*DF*), the ratio of peak test-pulse current with prepulse to peak (immediately preceding) test-pulse current without prepulse.

binant M2-muscarinic receptors were co-expressed with channels, application of the M2 agonist, carbachol (CCh), substantially attenuated N-type current elicited by a test pulse depolarization to 20 mV (*b*, *filled circle*) compared with control conditions (*a*, *filled circle*). This result demonstrates that co-expression of receptors and channels in HEK 293 cells reconstitutes a system in which recombinant M2-muscarinic receptors inhibit recombinant N-type channels, presumably via endogenous G-protein-mediated signaling pathways.

To determine whether this reconstituted form of inhibition matched the voltage-dependent inhibition observed in neurons, we first tested for the presence of classic, qualitative features of voltage-dependent G-protein inhibition. As in neurons, control N-type currents (*a*) were virtually identical during the test pulse, whether a strong prepulse to 100 mV was absent (*filled circle*) or present (*open circle*). Furthermore, inhibited currents (*b*) revealed two hallmarks of voltage-dependent inhibition in neurons: slowed activation during inhibition (*filled circle*), called "kinetic slowing" (Marchetti et al., 1986); and transient reversal of inhibition following strong depolarization (*open circle*), called "prepulse facilitation" (Grassi and Lux, 1989; Elmslie et al., 1990). Diary plots on the right illustrate a third hallmark of voltage-dependent inhibition, the concurrence of inhibition and prepulse facilitation. The top plot shows peak test pulse current with (*open circle*) and without (*filled circle*) a prepulse. The bottom plot reports the degree of facilitation (*DF*) defined as the ratio of peak test pulse currents (with prepulse ÷ without prepulse) (after Ikeda, 1991). Both inhibition and facilitation closely match the period of carbachol application.

Next, we examined whether the detailed voltage dependence of modulation in our system matched that observed in neurons (Fig. 2 *A*). We used a modified voltage protocol in which a prepulse between −100 and 120 mV accompanied each test pulse to 20 mV. For clarity, the voltage stimuli and elicited whole-cell currents for only three prepulse magnitudes are shown to the left. In neurons, voltage-dependent G-protein inhibition is more pronounced for inward currents at moderate depolarizations than for outward currents at strong depolarizations (Kasai and Aosaki, 1989; Bean, 1989). Likewise, in our system, carbachol inhibited inward prepulse currents (*Ip*) more strongly than outward prepulse currents. The complete relationship of peak prepulse current (*Ip*) to prepulse voltage (*Vp*), shown to the right, documents these features. In neurons, the degree of facilitation (*DF*) is a U-shaped function of *Vp* under control conditions (Jones and Marks, 1989; Ikeda, 1991), which shifts upward during G-protein inhibition (Ikeda, 1991). Similarly, in our system, peak test pulse current without carbachol was significantly reduced by a 20-mV prepulse (*b*), yet was hardly affected by an 80-mV prepulse (*c*). With carbachol, peak test pulse current was also diminished by a 20-mV prepulse (*b*), but was greatly potentiated by an 80-mV prepulse (*c*). As in neurons, the complete relationship of *DF* to *Vp* had a U-shape under control conditions (*bottom right, filled circles*), which shifted upward during M2-mediated inhibition (*bottom right, open circles*).

A final feature of voltage-dependent G-protein inhibition in neurons is a shift in the voltage-dependence of N-type channel activation to more depolarized potentials, without a reduction in the number of functional channels (Bean, 1989). In our system, tail currents following a family of test pulses shared this property (Fig. 2 *B*). Tail currents without carbachol (*filled circles*) activated at less depolarized potentials than those with carbachol (*open circles*). Maximal tail currents at strongly depolarized potentials were the same, regardless of carbachol, providing direct evidence for a purely voltage-dependent form of inhibition. Moreover, just as in neurons, tail activation curves could be represented as the sum of two Boltzmann functions whose relative amplitudes, but not slope and midpoint parameters, were affected by carbachol (smooth curves show fits). The lower and higher voltage Boltzmann components may correspond to pools of uninhibited ("willing") and G-protein inhibited ("reluctant") channels, respectively, suggesting that carbachol simply shifts channels into a pool requiring stronger depolarization to activate (Bean, 1989).

Though the results described in Figs. 1 and 2 demonstrate that reconstituted, M2-mediated inhibition possesses the detailed features of voltage-dependent G-protein inhibition in neurons, our measurements do not exclude the possibility that additional regulatory pathways may have contributed to the inhibition of N-type current, a feature that may be present in certain neurons (Bernheim et al., 1991; Boland and Bean, 1993; Luebke and Dunlap, 1994). The presence of multiple regulatory pathways that converge on N-type channels would complicate attempts to rigorously assess the effects of voltage-dependent inhibition in isolation. Fig. 3 *A* illustrates the potential complexity for our experimental

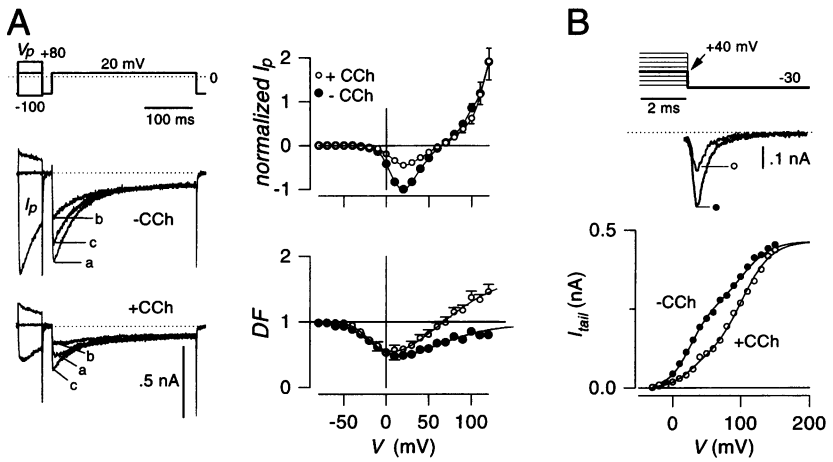

FIGURE 2 Voltage-dependent characteristics of carbachol inhibition of N-type Ca^{2+} channels. (*A*, *left*) voltage protocol and whole-cell currents before (*above*) and after (*below*) addition of carbachol (CCh). The prepulse and interpulse lasted 50 ms and 20 ms, respectively. Prepulse currents (*Ip*) for both conditions correspond to *Vp* of 100, −100, and 20 mV, top to bottom. Test-pulse currents for both conditions correspond to *Vp* of −100 (*a*), 20 (*b*), and 100 (*c*) mV. (*Top right*) peak *Ip* plotted as a function of *Vp*, before (●) and after (○) carbachol addition, from $n = 5$–7 cells. Before averaging, *Ip* for each cell was normalized to the current at *Vp* = 20 mV without carbachol. Error bars, plotted when larger than symbols, equal SEM here and throughout. (*Bottom right*) relationship of *DF* to *Vp* with carbachol present (○) or absent (●), from $n = 4$–12 cells. (*B*, *top*) voltage protocol and exemplar tail currents with (○) and without (●) carbachol. Test depolarizations lasted 20 ms. Data were sampled at 20-μs intervals, and filtered at 10 kHz (−3 dB, 4-pole Bessel). Series resistance was compensated for 2.4 of 4.0 MΩ. Specimen tail currents follow test depolarization to 40 mV, shown filtered at 7 kHz. (*Bottom*) tail current as a function of test pulse potential. Tail current was averaged for 200 μs, beginning 600 μs after the end of a 20-ms test pulse. Smooth curves are least-squares fits by the dual-Boltzmann function:

$$I_{tail} = I_{max}\{F/(1 + \exp[q_1(V_1 - V)/kT]) + (1 - F)/(1 + \exp[q_2(V_2 - V)/kT])\}$$

Both with and without carbachol, I_{max} = 464 pA, V_1 = 25.1 mV, V_2 = 101.6 mV, q_1 = 1.62 e^-, q_2 = 1.18 e^-, and kT has the usual meaning. Relative magnitudes of midpoint voltages of dual Boltzmann fits correspond well to reported values, and carbachol reduces the fractional contribution of the low-threshold component (*F*) from 0.53 to 0.19, in overall agreement with observations in neurons (Bean, 1989). Outward currents were completely blocked by 2 μM ω-conotoxin GVIA.

system. Pathway "a" represents voltage-dependent inhibition, believed to arise from direct interaction between G-proteins and the channel. Pathway "b" represents an alternate convergent pathway, also initiated by M2-receptor activation, which acts on the channel through a different signal transduction cascade. In neurons, such alternate pathways can involve activation of protein kinases, producing a form of "voltage-independent" current inhibition that is not transiently reversed by strong depolarization (Diversé-Pierluissi et al., 1995). In our system, further complexity might arise if endogenous muscarinic receptors, stimulated by carbachol, also act on N-type channels through direct ("c") or indirect ("d") signaling pathways.

Several lines of evidence suggest that our recombinant system reconstitutes a single, voltage-dependent modulatory pathway between homogeneous populations of M2 receptors and N-type channels. Convergent, voltage-independent pathways in neurons feature marked current attenuation during strong depolarization, a divergence of control and inhibited currents late in the test pulse, and a reduction of maximal tail current during inhibition (Luebke and Dunlap, 1994). We observed none of these effects (Fig. 2 *A*, *top right*; Fig. 2 *A*, *left*; and Fig. 2 *B*, respectively), arguing against the presence of a voltage-independent modulatory pathway ("b" in Fig. 3 *A*). Furthermore, characterization of cellular components involved in carbachol-evoked inhibition provided evidence against confounding interactions with endogenous signaling elements (Fig. 3 *B*). Carbachol failed to induce either inhibition or facilitation in cells transfected with recombinant channels, but not M2 (Fig. 3 *B*, *third column*), indicating that endogenous muscarinic receptors played no detectable role in the observed inhibition of N-type currents (thereby excluding "c" and "d" in Fig. 3 *A*). By comparison, M2 receptor activation by carbachol induced a degree of facilitation equal to that obtained during maximal G-protein activation by GTPγS (Fig. 3 *B*, first two columns). Hence, the only remaining possibility for our system is the voltage-dependent G-protein pathway ("a" in Fig. 3 *A*). M2 receptors couple to both PTX-sensitive Gi and PTX-insensitive Gq heterotrimeric G-proteins in HEK 293 cells (Offermanns et al., 1994). However, since overnight incubation of transfected cells with pertussis toxin (PTX, 500 ng/ml) eliminated both inhibition and facilitation, the βγ subunits (Herlitze et al., 1996; Ikeda, 1996) associated with α_i likely mediated the observed inhibition.

Unique effect of G-protein inhibition on single-channel gating

With assurance that the channel and modulatory pathway were known, we examined the kinetic basis of inhibition

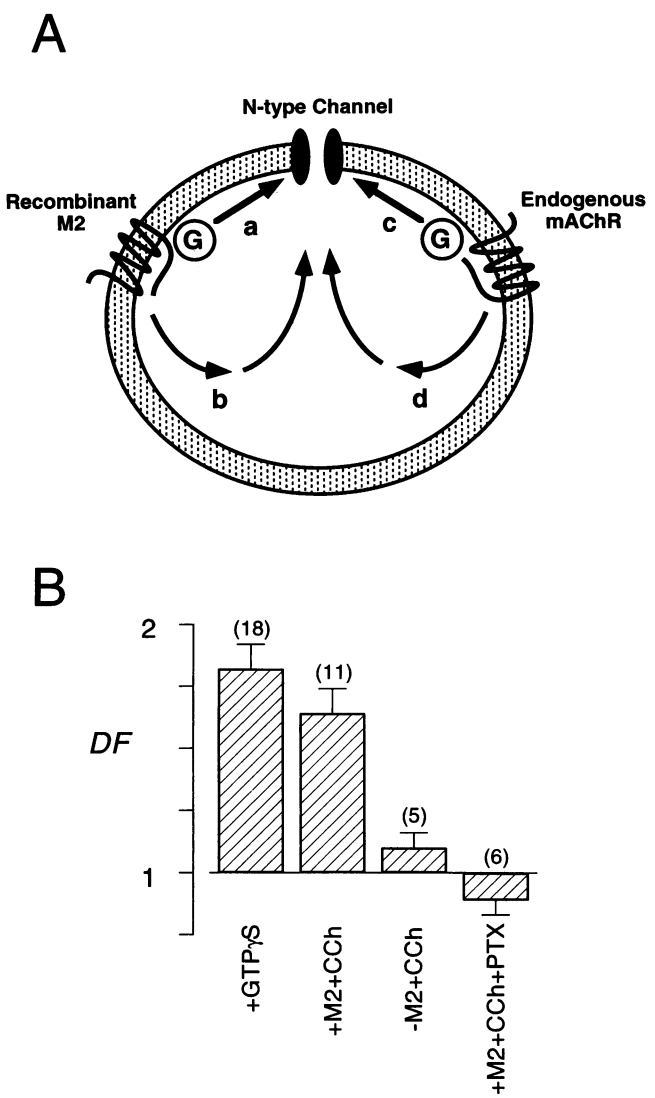

FIGURE 3 Absence of convergent pathways in N-type channel modulation. (*A*) Cartoon of potential pathways of carbachol-induced regulation of recombinant N-type channels. Pathways "a" and "c" represent direct G-protein modulation of the channel; pathways "b" and "d" represent G-protein mediated second messenger cascades. (*B*) Degree of facilitation (*DF*) observed during various perturbations of cellular signaling. Each bar plots *DF*, calculated as in Fig. 1 and averaged from the number of cells indicated. For all experiments, cells were transfected with N-type channels. Specific conditions were as follows (*left* to *right*): no M2 but GTPγS in internal solution; M2 co-transfected and carbachol present; no M2 but carbachol present; M2 co-transfected and carbachol present following PTX treatment.

and facilitation at the single-channel level (Fig. 4). Unitary N-type currents were recorded under two conditions. Under the first condition (Fig. 4, *A* and *C*), we omitted carbachol from the patch pipette to reveal gating behavior in the absence of appreciable G-protein inhibition. Under the second condition (Fig. 4, *B* and *D*), we included carbachol in the pipette to inhibit individual channels through M2 receptors isolated in the same patch of membrane (Delcour and Tsien, 1993). Identical stimulus protocols (Fig. 4 *A*, *top*) were used under both conditions. In the absence of carbachol, the prepulse had little effect on single-channel activity during the test pulse (Fig. 4 *A*), as expected from whole-cell records (Fig. 1 *A*). With or without a prepulse, channels generally activated quickly to a dense burst of activity and sometimes inactivated during the test pulse. The similarity of ensemble average currents with and without prepulse (Fig. 4 *A*, *bottom*) confirmed the lack of a prepulse effect on test pulse currents. In contrast, with carbachol in the pipette, the prepulse had a striking effect on overall channel activity during the test pulse (Fig. 4 *B*). Ensemble average currents (Fig. 4 *B*, *bottom*) clearly demonstrated inhibition and facilitation similar to that observed in whole-cell records (Fig. 1 *A*).

Close inspection of single-channel records gave the impression that a single change in elementary gating properties was ultimately responsible for both inhibition and facilitation. Carbachol produced a large increase in the time required for channels to first open following test pulse depolarization (first latency), which the prepulse reversed. However, once channels opened during the test pulse, the pattern of gating appeared to be the *same*, regardless of prepulse or carbachol exposure (compare Fig. 4 *A* and *B*). Durations of openings in the test pulse, following a prepulse or during carbachol exposure, remained constant. In patches without carbachol ($n = 5$), the mean open time was 0.29 ± 0.02 ms with prepulse, and 0.30 ± 0.02 ms without prepulse. In patches with carbachol ($n = 5$), the mean open time was 0.35 ± 0.05 ms with prepulse, and 0.35 ± 0.03 ms without prepulse. None of the differences were statistically significant ($p > 0.10$).

The idea that all features of modulation arise from changes in first latency, without changes in open times or subsequent channel gating, represents an important revision of prevailing hypotheses describing the elementary events underlying voltage-dependent G-protein inhibition of N-type channels (Delcour and Tsien, 1993; Delcour et al., 1993; Carabelli et al., 1996). To demonstrate unequivocally that changes in first latency alone gave rise to M2-mediated inhibition, we applied two quantitative tools to the single-channel data: first-latency analysis and conditional open-probability analysis (Imredy and Yue, 1994). First-latency distribution, $FL(t)$, is the probability that a channel first opens within a time t following membrane depolarization. Changes in characteristic first latencies appear as alterations to the shape or magnitude of *FL*. Conditional open probability, $P_{oo}(t)$, is the probability that a channel is open at a time t after it first opens during the test pulse. Changes in either open or closed times after initial opening during the test pulse result in alterations to P_{oo}. For channels dominated by a single open state, *FL* and P_{oo} jointly specify open probability throughout the test pulse (Yue et al., 1990). Hence, the two functions jointly provide a comprehensive, quantitative summary of all gating behavior. With these properties in mind, we expected that an effect on *FL* without any change in P_{oo} would be the quantitative result of channel modulation due to a change in first latency alone.

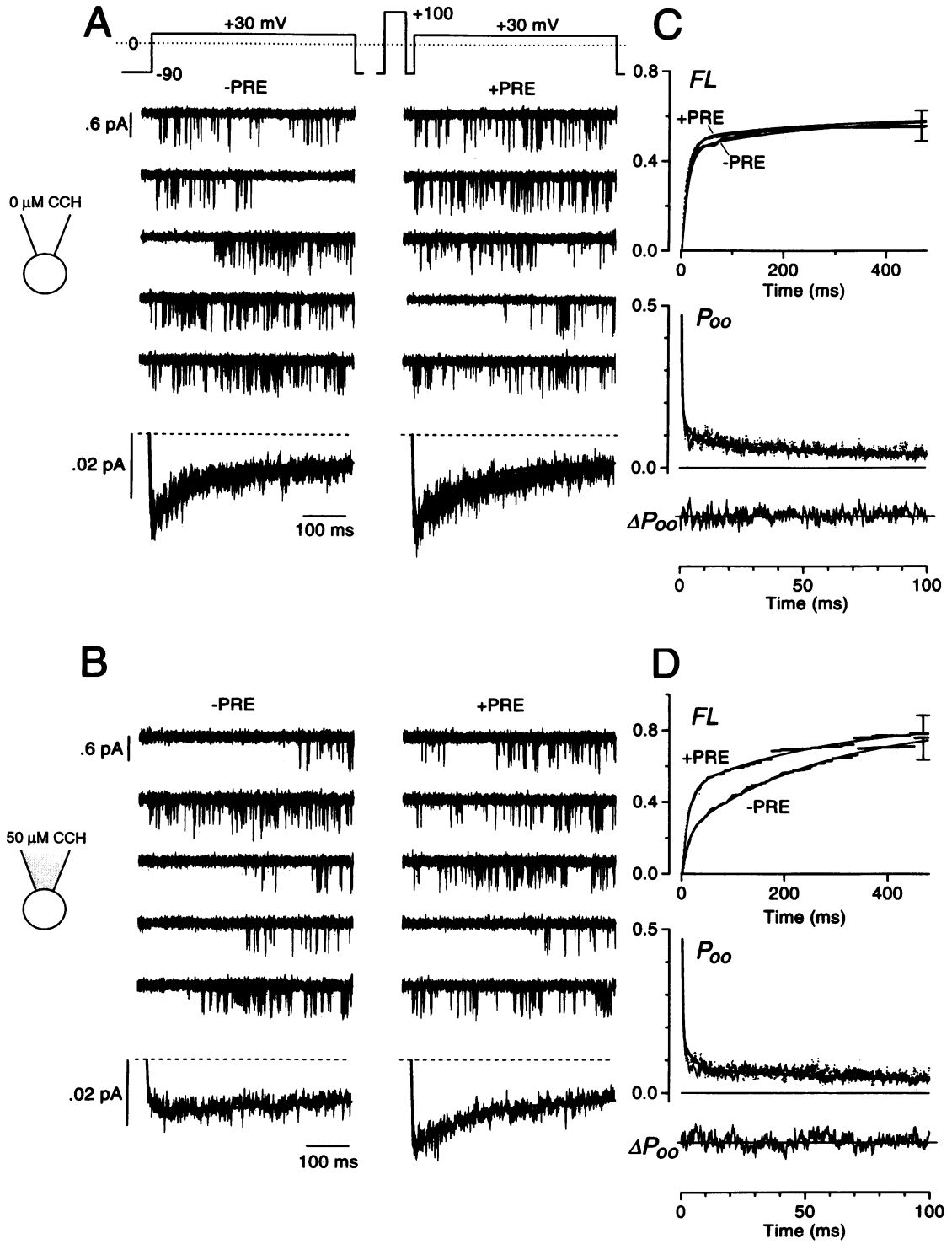

FIGURE 4 Kinetic basis of inhibition and facilitation at the single-channel level. (*A*, *top*) voltage protocol. Test pulses to 30 mV, delivered every 5 s, were alternately preceded by a 50-ms prepulse to 100 mV. (*Center*) exemplar records from a control patch without carbachol or M2 receptor. The charge carrier was 140 mM Ba^{2+}. Two channels were present, filtered at 1500 Hz. (*Bottom*) single-channel ensemble average current, averaged from 5 patches, each normalized by channel number. (*B*) Same format and voltage protocol as (*A*), but with M2 and carbachol. Exemplar patch contained 3 channels, filtered at 1500 Hz. Ensemble average calculated from 5 patches. (*C*) Quantitative analysis of control patches in (*A*). (*Top*) first latency distribution (*FL*) for current records with (+*PRE*) and without (−*PRE*) prepulse. (*Center*) conditional open probability (P_{oo}) with (*connected trace*) and without (*individual points*) prepulse, both plotted on the same axes. (*Bottom*) there was no statistical significance to the difference trace $\Delta P_{oo} = P_{oo}$ (with prepulse) $- P_{oo}$ (without prepulse) ($p > 0.40$, average *t*-statistic over entire period). *FL* and P_{oo} averaged from 5 patches in (*A*). *FL* plateau was 0.56 ± 0.07 with prepulse and 0.56 ± 0.07 without prepulse from $n = 5$ patches ($p > 0.10$). (*D*) Quantitative analysis of carbachol patches in (*B*), using same format as (*C*). *FL* and P_{oo} averaged from 5 patches in (*B*). *FL* plateau was 0.78 ± 0.10 with prepulse, and 0.80 ± 0.12 without, from $n = 5$ patches ($p > 0.10$). Smooth curve fits in (*C*) and (*D*) generated by the quantitative mechanism in Fig. 7 *B*. The same curve fits P_{oo} in (*C*) and (*D*).

Fig. 4 *C* shows the results of first-latency and conditional open-probability analyses of patches without carbachol. The quick rise of *FL* corresponds to rapid activation of channels, as observed in corresponding single-channel records (Fig. 4 *A*). The minute effect of the prepulse on *FL* probably reflects a small degree of basal G-protein activation, even in the absence of carbachol. P_{oo} functions with (*connected points*) and without (*individual points*) the prepulse are indistinguishable, as demonstrated by the zero-valued difference trace, ΔP_{oo}. The lack of any significant prepulse-induced change in *FL* or P_{oo}, under control conditions, confirms the generally small effect of prepulse depolarization on the gating of largely uninhibited N-type channels.

Quantitative analysis of patches with carbachol in the pipette provided the critical evidence for our simplified view of inhibition and facilitation (Fig. 4 *D*). The dearth of early openings (Fig. 4 *B*) introduces a prominent, slow component of activation into *FL*, as if activated G-proteins divide channels between inhibited (slowly activating) and uninhibited (rapidly activating) pools. The prepulse increased the fractional contribution of the fast component of *FL*, as if facilitation moved channels from one pool to the other. Despite major changes in the kinetics of activation, neither carbachol nor the prepulse had any statistically significant effect on the plateau value of *FL* ($p > 0.10$), suggesting that neither inhibition nor facilitation affected the fraction of functionally active channels (Bean et al., 1984). Furthermore, the conditional open probability for patches with carbachol not only was unaffected by the prepulse, but also was identical to that for control patches (fits through P_{oo} are the same in Fig. 4, *C* and *D*). This invariance of P_{oo} demonstrates that neither inhibition nor facilitation affects channel gating after first opening. Hence, quantitative analysis firmly establishes that voltage-dependent G-protein inhibition of N-type Ca^{2+} channels occurs through a profound increase in first latency alone. The existence of a single modulatory effect at the single-channel level further excludes the possibility of a functionally distinct, convergent modulatory pathway (e.g., pathway "b" in Fig. 3 *A*) in our reconstituted system.

Absence of change in single-channel permeation with G-protein inhibition

The ability to examine an isolated pathway of voltage-dependent G-protein inhibition at the single-channel level permitted direct evaluation of the proposal (Kuo and Bean, 1993) that a substantial portion of voltage-dependent inhibition results from a reduction in the flux of ions through individual, open channels (unitary current). According to this hypothesis, prepulse facilitation disinhibits channels not only by increasing open probability during the test pulse, but also by increasing unitary current magnitude. For the experiments reported in Fig. 4 *B*, single-channel records provide no indication of any increase in unitary current following the prepulse, despite substantial facilitation of current. However, just as changes in the Michaelis constant might not affect the turnover rate of an enzyme saturated by substrate, changes in permeation properties of N-type channels may be obscured when the channel pore is saturated by the high concentrations of Ba^{2+} (140 mM) normally used in single-channel recordings (Kuo and Bean, 1993).

We therefore examined the effect of prepulse facilitation on the magnitude of unitary currents during the test pulse, using only 10 mM Ba^{2+} as the charge carrier (Fig. 5). For this experiment, carbachol in the pipette inhibited N-type channels, and a voltage protocol identical to that in Fig. 4, but with test pulse magnitude set to 20 mV, elicited single-channel currents. Fig. 5 *A* shows current records and ensemble averages for an exemplar patch, without (*above*) and with (*below*) a strong prepulse. Despite clear-cut facilitation of ensemble average currents, channel openings during test pulses with prepulses appear no larger than those elicited by test pulses alone.

To address the issue quantitatively, we used amplitude histogram analysis of single-channel currents to obtain precise estimates of unitary current magnitudes. In pursuing this approach, we were careful to avoid slurring of gating transitions between open and closed levels (Yellen, 1984) by maintaining a wide, 5-kHz bandwidth throughout the analysis. The maintenance of sharp gating transitions provided a crucial analytic advantage. Because the open-channel noise of calcium channels is not appreciably different from background noise (Yue and Marban, 1990), the amplitude histograms could now be described as the sum of Gaussian distributions, each with the *same* variance as baseline noise in the absence of channel activity. A narrower bandwidth, while visually enhancing distinct components in the histogram, vastly complicates its mathematical description, ultimately leading to less-constrained estimates of unitary current magnitude.

Fig. 5 *B* shows the results of amplitude histogram analysis of the exemplar patch in Fig. 5 *A*. Amplitude histograms were generated from test pulse current records without (*above*) and with (*below*) a prepulse. "Active region" histograms (*jagged lines*) were accumulated from regions of unitary current records within 240 μs of a channel opening. "Baseline" histograms (not shown) were accumulated from regions at least 240 μs away from any opening. Baseline histograms were Gaussian-distributed with zero mean, as expected from background electronic noise. Given our wide bandwidth, scaled copies of the baseline histograms, shifted by multiples of the unitary current magnitude, i, sum together to comprise the active histograms. Maximum-likelihood fits of these summed Gaussian functions thereby provide highly constrained estimates of i (Hasselblad, 1966; Stricker and Redman, 1994). In Fig. 5 *B*, the smooth curves show overall fits, and the dashed curves show individual Gaussian components (centered at 0, i, and $2i$, as labeled). Amplitude histogram analysis indicates that the prepulse had no effect on unitary current magnitude for the exemplar patch, as demonstrated by overlapping 95% confidence intervals for i, determined by bootstrap estimation (Efron

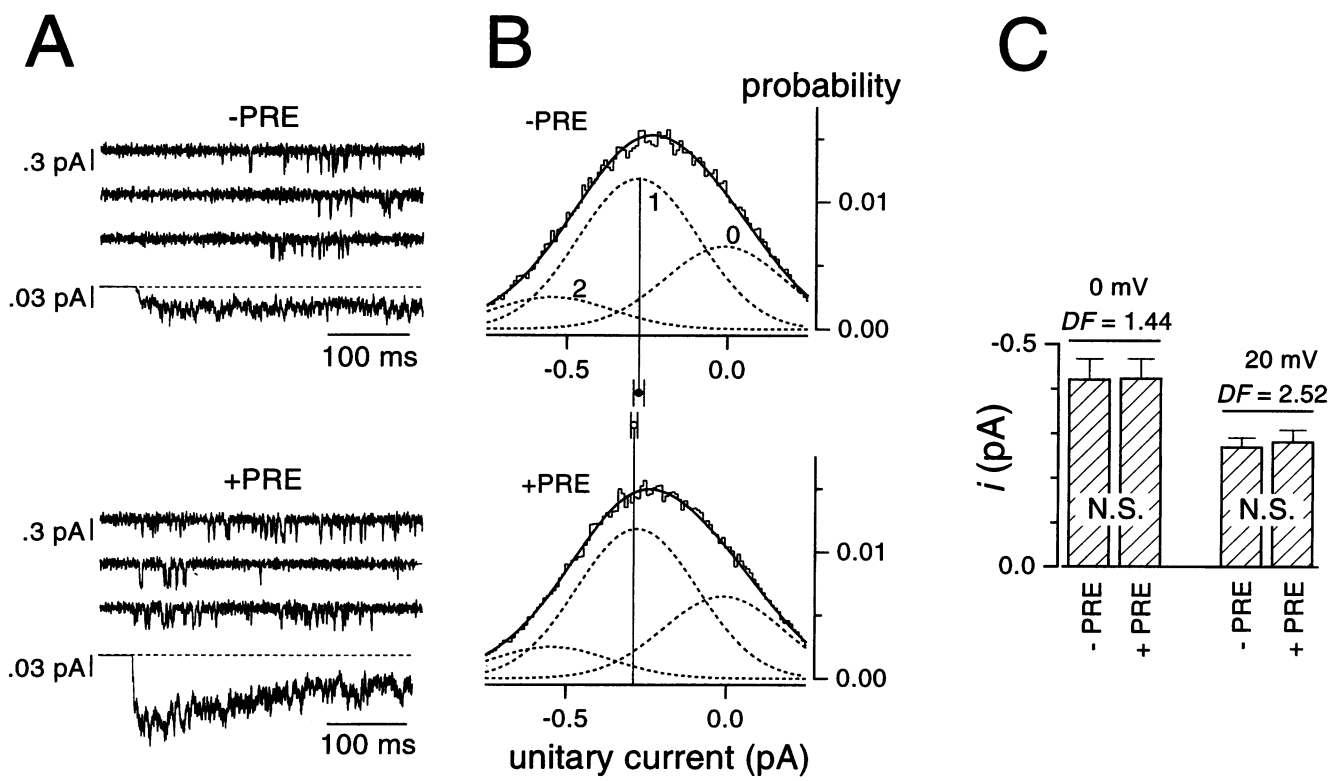

FIGURE 5 Invariance of permeation during prepulse facilitation. (*A*) Single-channel currents and ensemble averages of an exemplar patch, with carbachol and 10 mM Ba^{2+} in the patch pipette. Upper traces (*−PRE*) correspond to a 20-mV test pulse without prepulse, lower traces (*+PRE*) to the same test pulse preceded by a 50-ms prepulse to 100 mV. The patch contained 4 channels, filtered at 5 kHz during analysis, but shown at 1 kHz for clarity. Sampling rate was 25 kHz. (*B*) Amplitude histogram analysis of exemplar patch in (*A*). Each histogram was fit (*smooth curve*) by baseline noise components (*dashed curves*) centered at 0, *i*, and 2*i*. Error bars show 95% confidence intervals for *i*. (*C*) Estimates of *i* for test pulses to indicated voltages, with or without prepulse. Each voltage shows averaged data from $n = 3$ patches. Prepulse-induced changes were not significant (NS) throughout. *DF* indicates average degree of facilitation. In single-channel patches, *DF* was estimated from the fractional increase in the fast component of *FL* because peak ensemble average values were sometimes poorly defined. For the exemplar patch shown in Fig. 5 *A*, $DF \approx 3$.

and Tibshirani, 1993; Stricker et al., 1994). Statistical power calculation (Rosner, 1995) suggests that a change in *i* of even 7% would have been detectable at $p < 0.05$ for the same patch. We performed amplitude histogram analysis on six different patches at two test-pulse voltages. Not one of the patches exhibited any significant change in unitary current magnitude (Fig. 5 *C*, *p* ranging from 0.15 to 0.90), despite clear facilitation.

To directly examine the sensitivity of amplitude histogram analysis, we simulated single-channel records according to a kinetic model of inhibition fit to *FL*, P_{oo}, and ensemble average currents for the patch shown in Fig. 5 *A*. Simulated records possessed noise and filtering characteristics identical to those of the exemplar patch, and inhibited sweeps featured a 25% reduction in *i*, the minimum suggested by noise analysis of whole-cell currents (Kuo and Bean, 1993). Fig. 6 *A* displays simulated current records and ensemble average currents predicted by the model (*smooth curves*). To facilitate comparison, model predictions are shown superimposed upon ensemble average current records for the exemplar patch, and the format of the figure is identical to that of Fig. 5 *A*. Amplitude histogram analysis of these simulated records (Fig. 6 *B*) indicates that the minimum expected change in unitary current magnitude, 25%, would have been clearly detected ($p < 0.0001$) using our analysis technique. Hence, voltage-dependent G-protein inhibition seems unlikely to occur through a significant reduction in unitary current amplitude.

DISCUSSION

Our study demonstrates that co-expression of recombinant N-type channels and M2-muscarinic receptors in HEK 293 cells reconstitutes an isolated pathway of voltage-dependent G-protein inhibition of N-type channels. The experimental system provides an opportunity to pursue extensive single-channel investigation of the elementary events underlying this important form of N-type channel regulation. We find that voltage-dependent modulation exclusively arises from changes in first latency, the time required for a channel to first open following membrane depolarization. No further changes in gating or permeation are apparent. This simple, first-latency effect has direct implications for the mechanism through which G-proteins inhibit N-type channels, and stands in sharp contrast to previous proposals that G-pro-

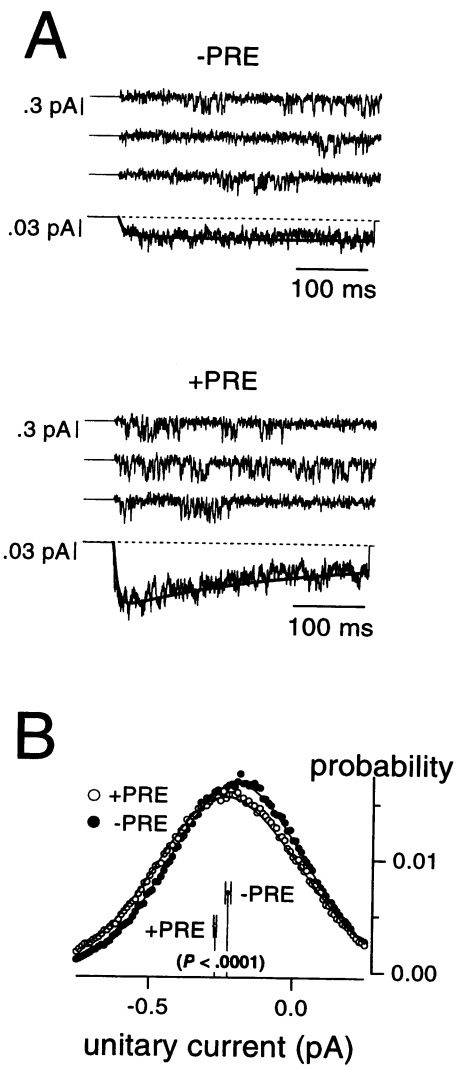

FIGURE 6 Sensitivity of amplitude histogram analysis by simulation. (*A*) Simulated single-channel activity. Format identical to that in Fig. 5 *A*, including sampling frequency and effective filtering. There are 4 simulated channels in the patch. The smooth curves are predicted ensemble average currents for simulated patch. Experimental ensemble average currents from Fig. 5 *A* are superimposed. (*B*) Amplitude histogram analysis of simulated channel records in which inhibited openings featured a 25% reduction in *i*. Simulated activity was generated by a kinetic mechanism (similar to that in Fig. 7 *B*) that was fit to the exemplar patch in (*A*). See Experimental procedures (Analysis of single-channel permeation) for details of the simulation. Disjoint 95% confidence intervals indicate that the reduction in *i* was clearly detected by our estimation method.

teins reduce unitary current amplitude (Kuo and Bean, 1993), or that G-proteins exert multiple effects on gating (Delcour and Tsien, 1993; Delcour et al., 1993).

Mechanistic implications of a change in first latency alone

To explore the mechanism underlying the observed effect on first latency, we considered different models of N-type channel behavior during voltage-dependent G-protein inhibition. The majority of these can be grouped into three classes (Fig. 7 *A*). Each class shares two widely accepted features that explain inhibition and facilitation in coarse outline. First, in each class, channels gate according to two groups of conformational states, called "willing" and "reluctant" modes (Bean, 1989). Current activation follows the movement of channels, from left to right, through a series of closed states (*C*) to one or a few open states (*O*). Differences in rate constants between conformational states ensure that channels in the reluctant mode are slower and less likely to open. Hence, inhibition with kinetic slowing results from the movement of channels from willing to reluctant modes (Boland and Bean, 1993). Conversely, facilitation results from the transient return of channels from reluctant to willing modes.

Second, G-protein binding to the channel either directly (Elmslie et al., 1990; Boland and Bean, 1993) or allosterically (Delcour and Tsien, 1993) induces a transition from the willing to the reluctant mode. Vertical transitions between modes are therefore tightly linked to G-protein (un)binding. The voltage dependence of modulation arises from the tendency of voltage to move G-protein-bound channels into conformations near the reluctant open state, where G-proteins unbind more rapidly (Elmslie et al., 1990; Boland and Bean, 1993), as indicated by lengthening up-arrows in the "permissive" and "preferential" exchange models. Transitions associated with G-protein binding and unbinding are generally assumed to be voltage independent.

The basis for deciding among the classes arises from fundamental differences in the rate of exchange between modes. Restricted exchange mechanisms (Kasai and Aosaki, 1989; Delcour and Tsien, 1993; Delcour et al., 1993) predict that channels begin and end the test pulse in the same mode. In contrast, permissive exchange mechanisms (Bean, 1989; Elmslie et al., 1990; Boland and Bean, 1992) allow some intermodal transitions during the test pulse. To the extent that willing (O) and reluctant (O′) openings occur, both restrictive and permissive mechanisms predict changes in P_{oo} with modulation (Sigworth, 1981; Imredy and Yue, 1994). Briefly, each open state contributes its own distinct component to P_{oo}, weighted by its share of first openings; hence, as the ratio of willing to reluctant first openings changes with modulation, the relative contribution of each component to P_{oo} would be expected to change, causing the overall shape of P_{oo} to be different. In addition, to the extent that exit rates from O and O′ differ, both restrictive and permissive mechanisms predict changes in average opening duration during modulation. Neither changes in P_{oo} nor changes in open times were observed experimentally.

We are therefore left with preferential exchange mechanisms. In this class, rate constants are arrayed such that it is far more probable for a reluctant channel to move upward into the willing mode than move across into the reluctant open state. As a result, channels in the reluctant mode almost always shift to the willing mode before opening during the test pulse. Though openings in the reluctant mode

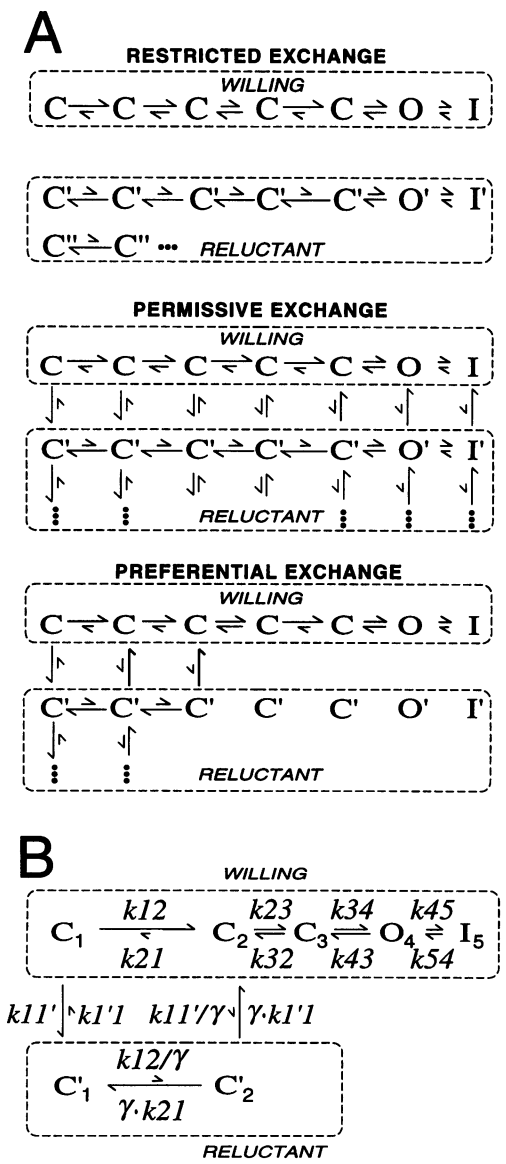

FIGURE 7 Mechanisms of G-protein inhibition. (*A*) Three proposed mechanisms of voltage-dependent G-protein inhibition of N-type Ca^{2+} channels. Capital letters (*C*, *O*, *I*) represent closed, open, and inactivated channel conformations; *arrows* represent transition rates between states; *dots* indicate that additional interconnected states may exist. Only the preferential exchange mechanism is consistent with invariant P_{oo}. In the restricted exchange mechanism, vertical arrows are omitted to indicate that transitions occur over several seconds, not during a single-test depolarization. (*B*) Minimal version of preferential exchange model. Kinetic scheme predicts all ensemble average currents, *FL*, and P_{oo} during inhibition and facilitation (Fig. 4, *smooth curves*). Functionally active channels begin test pulses in C_1 or C_1'; the fraction of active channels in C_1 at the beginning of the test pulse is f_W. Changes in f_W account for all effects of modulation. For control patches (Fig. 4, *A* and *C*), the prepulse increased f_W from 0.79 to 0.86, presumably indicating transient relief of basal inhibition. The fraction of functionally active channels, which underlie sweeps with openings, was 0.60, regardless of prepulse. With carbachol (Fig. 2 *B* and *D*), the prepulse substantially increased f_W from 0.32 to 0.60; the fraction of active channels was 0.85, regardless of prepulse. Rate constants, under all conditions, were (in ms^{-1}): k12 = 5.25; k21 = 0.00853; k23 = 0.118; k32 = 0.150; k34 = 0.473; k43 = 2.28; k45 = 0.0763; k54 = 0.00197; k11′ = 0.0291; k1′1 = 0.00036. Negative cooperativity between voltage activation and G-protein binding, γ = 13.56.

(O′) are not strictly prohibited, they are exceedingly unlikely. Due to the absence of appreciable reluctant openings, preferential exchange mechanisms are consistent with the observed change in first latency alone, without changes in P_{oo} or open times.

Furthermore, a minimal preferential exchange model (Fig. 7 *B*) accurately predicts all gating properties observed in single-channel patches. In this model, we omit reluctant states like C_3', O_4', and I_5', because they are exceedingly unlikely to be occupied. Smooth fits through ensemble average currents, first-latency distributions, and conditional open-probability functions throughout Fig. 4 demonstrate the extensive predictive power of the model. Remarkably, changes in a *single* parameter of the model, the probability of beginning the test pulse in the willing mode (state C_1) versus the reluctant mode (state C_1'), fully account for all effects of inhibition and facilitation. No changes in any transition rate constants are required. The model indicates that, on average, inhibition reduces the fraction of willing channels from 80% to 30%, while facilitation restores the fraction to 60%.

The impressive fit of the preferential exchange model to the data encourages consideration of several predictions about the link between G-protein binding and N-type channel gating. First, if willing-to-reluctant transitions correspond to G-protein binding, the model requires that G-proteins unbind before the channel opens during the 30-mV test pulse (with 140 mM Ba^{2+} as charge carrier). This voltage corresponds to the peak of the N-type channel current-voltage relationship (Boland et al., 1994), or about 0 mV in physiological saline (with 2.5 mM Ca^{2+} as charge carrier) (Golard and Siegelbaum, 1993). At more negative voltages, the tendency for channels to shift from reluctant to willing modes before opening is likely to become even more pronounced (Elmslie and Jones, 1990; Boland and Bean, 1993). Hence, the prediction of G-protein unbinding before channel opening pertains to a large portion of the physiologically relevant voltage range.

Second, the preferential exchange model predicts that once channels move from reluctant to willing modes, G-proteins do not rebind to the channel. The lack of rebinding occurs because rate constants in the willing mode strongly favor rightward movement toward the open state. Hence, once a channel escapes from the reluctant mode, it is rapidly sequestered in states that either cannot bind G-proteins (C_3, O_4, I_5), or do not favor rebinding (C_2). After membrane repolarization, rebinding occurs, since voltage-dependent transitions change to favor states (C_1) with high affinity for G-proteins.

Independent experimental support for this prediction arises from our data. In the absence of rebinding, channels ultimately pool in the willing mode, particularly by the end of a long test pulse. Hence, currents at the end of long depolarizations are predicted to be independent of both the prepulse and the extent of G-protein inhibition, since they are determined by an equilibrium distribution among states like C_2, C_3, O_4, and I_5. Conversely, if G-proteins do rebind,

channels divide between reluctant and willing modes, even late in the test pulse. Inhibited currents measured at the end of prolonged depolarizations would then be predicted to be smaller than control currents. The convergence of actual control and modulated currents late in the test pulse (Fig. 8 *A*) is therefore inconsistent with G-protein rebinding. Further evidence against G-protein rebinding comes with the insensitivity of both P_{oo} (Fig. 4) and transition rate constants (Fig. 7 *B*) to channel modulation. If G-proteins appreciably rebind, carbachol should introduce an additional decay component into P_{oo}, due to the increased number of G-protein-bound states a channel can visit after first opening. However, P_{oo} was unaffected by modulation. Likewise, rate constants corresponding to G-protein binding should be larger when carbachol application increases the number of active G-proteins. Since there was no need to adjust these rates between fits of control and inhibited data in Fig. 4, it is likely that channels rarely reside in states (e.g., C_1) where G-proteins appreciably rebind.

A third prediction of the preferential exchange model is that G-protein modulation is likely to affect the movement of channel gating charge in the membrane. Because G-proteins trap channels in deep closed states (C_1'), the gating charge movement of inhibited channels should be slowed, or perhaps immobilized. Following prepulse facilitation, the slowed or immobilized charge ought to be transiently released. Our recombinant system enables direct tests of this prediction.

Relation to previous studies

We are not the first to propose a preferential exchange mechanism (Fig. 7) for voltage-dependent G-protein inhibition of N-type channels. Previously published quantitative models (Elmslie and Jones, 1990; Boland and Bean, 1993) predict preferential exchange behavior during modest depolarizations and permissive exchange behavior during stronger depolarizations. At weakly depolarized potentials, the voltage-independent (upward) transition rates between reluctant and willing modes exceed the voltage-dependent (rightward) transition rates between reluctant states. The relative magnitudes of these rate constants make the rightward movement of channels through reluctant states so slow and improbable that vertical escape to the willing mode almost always occurs before the reluctant open state can be reached. However, during sufficiently strong depolarizations, voltage-dependent transition rates exceed voltage-independent rates, and the balance shifts. Under this condition, the rightward movement of reluctant channels is favored to the point that the reluctant open state may be visited before escape to the willing mode. Until now, experimental evidence for either permissive or preferential behavior has been indirect, and the voltage range in which channels switch between the two classes of behavior has been unclear.

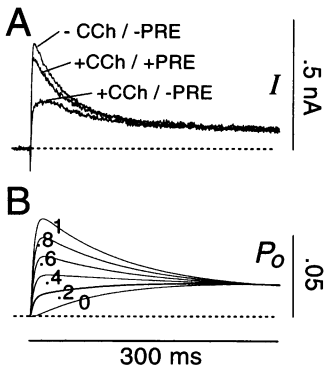

FIGURE 8 Predictions of the preferential exchange mechanism. (*A*) Convergence of whole-cell test pulse currents during prolonged depolarization to 20 mV. Currents shown inverted for comparison with (*B*). Voltage protocol and conditions as in Fig. 2 *A*; prepulse to 100 mV as indicated (+*PRE*). (*B*) Open probability predicted by the preferential exchange model (Fig. 7 *B*). Numbers indicate fraction of willing channels at the start of the test pulse. All channels were assumed to be functionally active.

The striking aspect of this study is the explicit, single-channel evidence that preferential exchange dominates up to voltages as high as 0 mV under physiological conditions (30 mV with 140 mM Ba^{2+}). Hence, our results suggest that the number of reluctant openings is negligible over much of the voltage range spanned by neuronal action potentials (−70 to 30 mV; Borst et al., 1995). A simple model of preferential exchange, such as in Fig. 7 *B*, therefore may suffice to represent N-type channel gating and modulation over the range of physiological voltages.

The lack of reluctant openings elicited by our voltage protocols may therefore explain the absence of any detectable change in unitary current amplitude during G-protein inhibition and facilitation (Fig. 5). If reluctant openings have smaller unitary current, as a previous report suggests (Kuo and Bean, 1993), we would not detect it, simply because no reluctant openings were present in our experiments. We emphasize, however, that our data do firmly exclude G-protein-induced changes in permeation over most of the physiologically relevant voltage range. We performed amplitude histogram analysis on current records acquired at 20 mV with 10 mM Ba^{2+} in the pipette, corresponding to a depolarization magnitude of 5 mV under physiological conditions (T. P. Snutch, unpublished data). Hence, we seem to refute the suggestion that nearly half of current inhibition in this voltage range is attributable to reduced unitary current (Kuo and Bean, 1993).

It may be possible to force reluctant channels into the reluctant open state using a very strong prepulse (≥100 mV) that lasts only a few milliseconds (Boland and Bean, 1993). Amplitude histogram analysis of openings immediately following the prepulse might then allow measurement of the unitary currents of reluctant openings. However, the physiological significance of such prepulse-induced openings would require careful assessment.

Our results contrast most strongly with previous reports (Delcour and Tsien, 1993; Delcour et al., 1993) concerning the effects of G-protein inhibition on single-channel gating.

These extensive studies of single-channel currents in neurons suggest that activated G-proteins alter the prevalence of three distinct gating modes. Our data provide no visual indication that N-type channel gating follows such modes. Furthermore, such a proposal is incompatible with the invariance of P_{oo} and the large change in *FL* that we observe. Shifts in the distribution of channels among different gating modes should have altered the appearance of P_{oo}, which consists of a weighted mixture of P_{oo} components from each mode (Imredy and Yue, 1994). Finally, the absence of any reported effects of channel modulation on first latency clearly differ from the profound changes in first latency that we observe. It is possible that these previous studies in neurons misidentified another Ca^{2+} channel type as the N-type channel (Elmslie et al., 1994).

Our findings also differ significantly from a more recent single-channel study (Carabelli et al., 1996). In agreement with our findings, this study suggests that G-proteins markedly delay first-channel openings. However, the study also reports changes in the pattern of gating following the first opening, as reflected by a one-third reduction in open probability between first and last openings. This substantial reduction in open probability would be clearly detected as a difference in P_{oo} for inhibited and uninhibited channels. The discrepancy with our findings may be explained by the presence of convergent modulatory pathways (Fig. 3 *A*) in IMR32 cells, as detected by Carabelli et al. (1996).

Insights into N-type channel physiology

This study reveals that a simple delay in the first opening of individual channels, resulting from G-protein inhibition, produces complex alterations in the waveform of whole-cell currents. Simulations of the minimal preferential exchange model in Fig. 7 *B* illustrate the enormous effect of changes in first latency on whole-cell behavior. Incremental changes in the probability of beginning the test pulse in the willing (C_1) versus the reluctant (C_1') mode produce a broad spectrum of simulated waveforms (Fig. 8 *B*), which are reminiscent of actual current records (Fig. 8 *A*). Changes in whole-cell activation and inactivation rates both result from underlying modulation of first latency. In addition, rates of activation in macroscopic current records poorly reflect the extent of G-protein inhibition at the single-channel level: nearly half of the channels need to be inhibited before substantial kinetic slowing appears. Such simulations refine the link between modulation of macroscopic currents and the true extent of inhibition at the single-channel level.

Finally, our study raises intriguing possibilities for the behavior of individual channels during neuronal action potentials. Because the first latencies of even uninhibited N-type channels may be long compared with the 1–3-ms duration of action potentials (Borst et al., 1995), the probability that any individual channel opens at all during an action potential could be quite low. This may importantly contribute to the high failure rate of synaptic transmission (Hessler et al., 1993). By increasing first latency 10-fold, G-proteins may effectively switch-off channels during the brief duration of an action potential. Therefore, when N-type channels manage to activate, the limited duration of the action potential may only permit one or a few openings to occur. Hence, Ca^{2+} entry into the presynaptic terminal could very well appear as "calcium sparks" (Cheng et al., 1993), with the number of sparks scaling linearly with the degree of G-protein inhibition.

We thank E. G. Peralta and K. P. Campbell for clones, J. G. Mulle and W. Guo for technical assistance, and D. L. Brody, K.-W. Yau, and N. C. Yue for discussion and comments. Supported by a NSF Presidential Faculty Fellowship (D.T.Y.), the MRC of Canada and the Howard Hughes Medical Institute (T.P.S.), and a National Institutes of Health Medical Scientist Training Program Award (P.G.P.).

REFERENCES

Bean, B. 1989. Neurotransmitter inhibition of neuronal calcium currents by changes in channel voltage dependence. *Nature.* 340:153–156.

Bean, B. P., M. C. Nowycky, and R. W. Tsien. 1984. β-adrenergic modulation of calcium channels in frog ventricular heart cells. *Nature.* 307:371–375.

Bernheim, L., D. J. Beech, and B. Hille. 1991. A diffusable second messenger mediates one of the pathways coupling receptors to calcium channels in rat sympathetic neurons. *Neuron.* 6:859–867.

Boland, L. M., and B. P. Bean. 1993. Modulation of N-type calcium channels in bullfrog sympathetic neurons by luteinizing hormone-releasing hormone: kinetics and voltage dependence. *J. Neurosci.* 13: 516–533.

Boland, L. M., J. A. Morrill, and B. P. Bean. 1994. ω-Conotoxin block of N-type calcium channels in frog and rat sympathetic neurons. *J. Neurosci.* 14:5011–5027.

Borst, J. G. G., F. Helmchen, and B. Sakmann. 1995. Pre- and postsynaptic whole-cell recordings in the medial nucleus of the trapezoid body of the rat. *J. Physiol. (Lond.).* 489:825–840.

Bourinet, E., T. W. Soong, A. Stea, and T. P. Snutch. 1996. Determinants of the G-protein dependent opioid modulation of neuronal calcium channels. *Proc. Natl. Acad. Sci. USA.* 93:1486–1491.

Carabelli, V., M. Lovallo, V. Magnelli, H. Zucker, and E. Carbone. 1996. Voltage-dependent modulation of single N-type Ca^{2+} kinetics by receptor agonists in IMR32 cells. *Biophys. J.* 70:2144–2154.

Chen, L., and L. Y. Huang. 1992. Protein kinase C reduces Mg^{2+} block of NMDA-receptor channels as a mechanism of modulation. *Nature.* 356: 521–523.

Cheng, H., W. J. Lederer, and M. D. Cannell. 1993. Calcium sparks: elementary events underlying excitation-contraction coupling in heart muscle. *Science.* 262:740–744.

Delcour, A. H., D. Lipscombe, and R. W. Tsien. 1993. Multiple modes of N-type calcium channel activity distinguished by differences in gating kinetics. *J. Neurosci.* 13:181–194.

Delcour, A. H., and R. W. Tsien. 1993. Altered prevalence of gating modes in neurotransmitter inhibition of N-type calcium channels. *Science.* 259:980–984.

Dhallan, R. S., K.-W. Yau, K. A. Schrader, and R. R. Reed. 1990. Primary structure and functional expression of a cyclic nucleotide-activated channel from olfactory neurons. *Nature.* 347:184–187.

Diversé-Pierluissi, M., P. K. Goldsmith, and K. Dunlap. 1995. Transmitter-mediated inhibition of N-type calcium channels in sensory neurons involves multiple GTP-binding-proteins and subunits. *Neuron.* 14: 191–200.

Dubel, S. J., T. V. Starr, J. Hell, M. K. Ahlijanian, J. J. Enyeart, W. A. Catterall, and T. P. Snutch. 1992. Molecular cloning of the alpha subunit of an omega-conotoxin-sensitive calcium channel. *Proc. Natl. Acad. Sci. USA.* 89:5058–5062.

Dunlap, K., J. I. Luebke, and T. J. Turner. 1995. Exocytotic Ca^{2+} channels in mammalian central neurons. *Trends Neurosci.* 18:89–98.

Efron, B., and R. Tibshirani. 1993. An Introduction to the Bootstrap. Chapman and Hall, New York. 45–49.

Elmslie, K. S., P. J. Kammermeier, and S. W. Jones. 1994. Reevaluation of Ca^{2+} channel types and their modulation in bullfrog sympathetic neurons. *Neuron.* 13:217–218.

Elmslie, K. S., W. Zhou, and S. W. Jones. 1990. LHRH and GTP-γ-S modify calcium current activation in bullfrog sympathetic neurons. *Neuron.* 5:75–80.

Golard, A., and S. A. Siegelbaum. 1993. Kinetic basis for the voltage-dependent inhibition of N-type calcium current by somatostatin and norepinephrine in chick sympathetic neurons. *J. Neurosci.* 13: 3884–3894.

Grassi, F., and H. D. Lux. 1989. Voltage-dependent GABA-induced modulation of calcium currents in chick sensory neurons. *Neurosci. Lett.* 105:113–119.

Hasselblad, V. 1966. Estimation of parameters for a mixture of normal distributions. *Technometrics.* 8:431–444.

Herlitze, S., D. E. Garcia, K. Mackie, B. Hille, T. Scheuer, and W. A. Catterall. 1996. Modulation of Ca^{2+} channels by G-protein βγ subunits. *Nature.* 380:258–262.

Hessler, N. A., A. M. Shirke, and R. Malinow. 1993. The probability of transmitter release at a mammalian central synapse. *Nature.* 366: 569–572.

Hille, B. 1994. Modulation of ion-channel function by G-protein-coupled receptors. *Trends Neurosci.* 17:531–536.

Ikeda, S. 1991. Double-pulse calcium channel facilitation in adult rat sympathetic neurons. *J. Physiol. (Lond.).* 439:181–214.

Ikeda, S. 1996. Voltage-dependent modulation of N-type calcium channels by G-protein βγ subunits. *Nature.* 380:255–258.

Imredy, J. P., and D. T. Yue. 1992. Submicroscopic Ca^{2+} diffusion mediates inhibitory coupling between individual Ca^{2+} channels. *Neuron.* 9:197–207.

Imredy, J. P., and D. T. Yue. 1994. Mechanism of Ca^{2+}-sensitive inactivation of L-type Ca^{2+} channels. *Neuron.* 12:1301–1318.

Jones, S. W., and T. N. Marks. 1989. Calcium currents in bullfrog sympathetic neurons. II. Inactivation. *J. Gen. Physiol.* 94:169–182.

Kasai, H., and T. Aosaki. 1989. Modulation of Ca^{2+} channel current by an adenosine analog mediated by a GTP-binding protein in chick sensory neurons. *Pfluegers Arch.* 414:145–149.

Kuo, C.-C., and B. P. Bean. 1993. G-protein modulation of ion permeation through N-type calcium channels. *Nature.* 365:258–262.

Luebke, J. I., and K. Dunlap. 1994. Sensory neuron N-type calcium currents are inhibited by both voltage-dependent and -independent mechanisms. *Pfluegers Arch.* 428:499–507.

Marchetti, C., E. Carbone, and H. D. Lux. 1986. Effects of dopamine and noradrenaline on Ca channels of cultured sensory and sympathetic neurons of chick. *Pfluegers Arch.* 406:104–111.

Miller, R. J. 1990. Receptor-mediated regulation of calcium channels and neurotransmitter release. *FASEB J.* 4:3291–3299.

Offermanns, S., T. Wieland, D. Homann, J. Sandmann, E. Bombien, K. Spicher, G. Schultz, and K. H. Jakobs. 1994. Transfected muscarinic acetylcholine receptors selectively couple to G_i-type G-proteins and G_{q11}. *Mol. Pharmacol.* 45:890–898.

Peralta, E., A. Ashkenazi, J. W. Winslow, J. Ramachandran, and D. J. Capon. 1988. Differential regulation of PI hydrolysis and adenylyl cyclase by muscarinic receptor subtypes. *Nature.* 334:434–437.

Peralta, E. G., J. W. Winslow, G. L. Peterson, D. H. Smith, A. Ashkenazi, J. Ramachandran, M. I. Schimerlik, and D. J. Capon. 1987. Primary structure and biochemical properties of an M2 muscarinic receptor. *Science.* 236:600–605.

Pollo, A., M. Lovallo, E. Sher, and E. Carbone. 1992. Voltage-dependent noradrenergic modulation of omega-conotoxin-sensitive Ca^{2+} channels in human neuroblastoma IMR32 cells. *Pfluegers Arch.* 422:75–83.

Pragnell, M., J. Sakamoto, S. D. Jay, and K. P. Campbell. 1991. Cloning and tissue-specific expression of the brain calcium channel beta-subunit. *FEBS Lett.* 291:253–258.

Rosner, B. 1995. Fundamentals of Biostatistics. Duxbury Press, New York. 283–286.

Sigworth, F. J. 1981. Covariance of nonstationary sodium current fluctuations at the node of Ranvier. *Biophys. J.* 34:111–133.

Stanley, E. F. 1993. Single calcium channels and acetylcholine release at a presynaptic nerve terminal. *Neuron.* 11:1007–1011.

Stricker, C., and S. Redman. 1994. Statistical models of synaptic transmission evaluated using the expectation-maximization algorithm. *Biophys. J.* 67:656–670.

Stricker, C., S. Redman, and D. Daley. 1994. Statistical analysis of synaptic transmission: model discrimination and confidence limits. *Biophys. J.* 67:532–547.

Tomlinson, W. J., A. Stea, E. Bourinet, P. Charnet, J. Nargeot, and T. P. Snutch. 1993. Functional properties of a neuronal class C L-type calcium channel. *Neuropharmacology.* 32:1117–1126.

Wickman, K., and D. E. Clapham. 1995. Ion channel regulation by G-proteins. *Physiol. Rev.* 75:865–885.

Wilding, T. J., M. D. Womack, and E. W. McCleskey. 1995. Fast, local signal transduction between the mu opioid receptor and Ca^{2+} channels. *J. Neurosci.* 15:4124–4132.

Yellen, G. 1984. Ionic permeation and blockade in Ca^{2+} -activated K^+ channels of bovine chromaffin cells. *J. Gen. Physiol.* 84:157–186.

Yue, D. T., P. H. Backx, and J. P. Imredy. 1990. Calcium-sensitive inactivation in the gating of single calcium channels. *Science.* 250: 1735–1738.

Yue, D. T., and E. Marban. 1990. Permeation in the dihydropyridine-sensitive calcium channel: multi-ion occupancy but no anomalous mole-fraction effect between Ba^{2+} and Ca^{2+}. *J. Gen. Physiol.* 95:911–939.